ORIGINAL ARTICLE

Journal of Cachexia, Sarcopenia and Muscle (2021)
Published online in Wiley Online Library (wileyonlinelibrary.com) **DOI:** 10.1002/jcsm.12813

RIPK3-mediated cell death is involved in DUX4-mediated toxicity in facioscapulohumeral dystrophy

Virginie Mariot[1†], Romain Joubert[1,2†], Laura Le Gall[1], Eva Sidlauskaite[1], Christophe Hourde[3], William Duddy[4], Thomas Voit[1], Maximilien Bencze[5,6] & Julie Dumonceaux[1,4*]

[1]*NIHR Biomedical Research Centre, University College London, Great Ormond Street Institute of Child Health and Great Ormond Street Hospital NHS Trust, London, UK;* [2]*United Kingdom Dementia Research Institute Centre, Maurice Wohl Clinical Neuroscience Institute, Institute of Psychiatry, Psychology and Neuroscience, King's College London, London, UK;* [3]*Laboratoire Interuniversitaire de Biologie de la Motricité, Université Savoie Mont Blanc, Chambéry, France;* [4]*Northern Ireland Center for Stratified/Personalised Medicine, Biomedical Sciences Research Institute, Ulster University, Derry~Londonderry, Northern Ireland, UK;* [5]*University Paris Est Créteil, INSERM, IMRB, Créteil, France;* [6]*The Dubowitz Neuromuscular Centre, Molecular Neurosciences Section, Developmental Neurosciences Programme, UCL Great Ormond Street Institute of Child Health, London, UK*

Abstract

Background Facioscapulohumeral dystrophy (FSHD) is caused by mutations leading to the aberrant expression of the DUX4 transcription factor in muscles. DUX4 was proposed to induce cell death, but the involvement of different death pathways is still discussed. A possible pro-apoptotic role of DUX4 was proposed, but as FSHD muscles are characterized by necrosis and inflammatory infiltrates, non-apoptotic pathways may be also involved.

Methods We explored DUX4-mediated cell death by focusing on the role of one regulated necrosis pathway called necroptosis, which is regulated by RIPK3. We investigated the effect of necroptosis on cell death *in vitro* and *in vivo* experiments using RIPK3 inhibitors and a RIPK3-deficient transgenic mouse model.

Results We showed *in vitro* that DUX4 expression causes a caspase-independent and RIPK3-mediated cell death in both myoblasts and myotubes. *In vivo*, *RIPK3*-deficient animals present improved body and muscle weights, a reduction of the aberrant activation of the DUX4 network genes, and an improvement of muscle histology.

Conclusions These results provide evidence for a role of RIPK3 in DUX4-mediated cell death and open new avenues of research.

Keywords FSHD; DUX4; Necroptosis; Ripk3; Facioscapulohumeral dystrophy

Received: 4 September 2020; Revised: 14 June 2021; Accepted: 7 September 2021
**Correspondence to: Dr. Julie Dumonceaux, Translational Myology Laboratory, Developmental Neurosciences, UCL Great Ormond Street Institute of Child Health, 30 Guilford Street, London WC1N 1EH, UK. Phone: +44 (0)2079052860, Email: j.dumonceaux@ucl.ac.uk*
[†]*These authors contributed equally to this work.*

Introduction

Facioscapulohumeral dystrophy (FSHD) is characterized by a loss of repressive epigenetic marks within the D4Z4 microsatellite located in the sub-telomeric region of chromosome 4.[1–3] In muscle, this chromatin relaxation, when associated with a permissive chromosome 4 carrying the ATTAAA polyadenylation signal, results in the expression of the DUX4 transcription factor whose ORF is present in each D4Z4 repeat, resulting in a poison protein effect through induction of multiple downstream genes.[4,5] DUX4 expression is extremely low, but it has been robustly found in adult and foetal FSHD muscle cells and biopsies.[6–8] DUX4 was proposed to disrupt multiple cellular functions (for review, see DeSimone *et al*.[9]) and to induce cell death in different models. Several publications have reported DUX4-mediated cell death *in vitro* in murine C2C12 or human myotubes[10–12] and *in vivo* in different species including mice.[13,14] However, the mechanisms leading to cellular death still need to be deciphered, and the involvement of p53-mediated apoptosis has been discussed.[13,15] Recently, DUX4 was also described to cause pathological accumulation of hyaluronic acid leading to

caspase-3/7 activation and cell death,[16] to lead to cytotoxicity mediated by a global accumulation of acetylated histone H3 that can be improved by the addition of specific p300 inhibitors,[17] and to activate the cellular hypoxia signalling pathway responsible for cell death.[18]

Here, we investigated the role of regulated necrosis in DUX4-mediated toxicity. Indeed, the concept of cell death has considerably evolved over the past 20 years, and cell death can be divided in non-programmed cell death or necrosis, which mainly occurs in response to accidental cell death, as opposed to programmed cell death, which is composed of autophagy, apoptosis, and programmed/regulated necrosis (for review, see previous works[19,20]). We focused on the most studied form of regulated necrosis called necroptosis, which has emerged as a major pathological process in many diseases including neurologic, cardiovascular, pulmonary, and gastrointestinal systems (for review, see Khoury *et al*.[20]). Necroptosis was initially defined as a receptor-interacting protein kinases 1 and 3 (RIPK1 and RIPK3)-dependent molecular cascade that is regulated by multiple steps of post-transcriptional modifications including phosphorylation and ubiquitination,[21] leading in particular to the pseudokinase mixed-lineage kinase domain-like (MLKL) phosphorylation and its translocation to the membrane and the disruption of the plasma membrane (for review, see Silke *et al*.[22]). Here, we show that necroptosis contributes to DUX4-mediated toxicity both *in vitro* and *in vivo*. We used the iC2C12-DUX4 cells that carry a doxycycline (dox)-inducible DUX4 transgene[10] and observed that DUX4 expression causes a RIPK1-mediated or a RIPK3-mediated necroptosis in either iC2C12-DUX4 myoblasts or myotubes, respectively. *In vivo*, the cre-inducible DUX4 transgenic mouse model[23] deficient in RIPK3[24] had reduced muscle and body weight loss following *DUX4* expression, a reduced activation of DUX4 network genes, and an improved muscle histology. This study thus provides evidence for a key role of necroptosis in DUX4-mediated cell death.

Methods

Animals housing and crosses

Mice were bred in the Biological Services Unit of the Great Ormond Street Institute of Child Health and University College London in accordance with the Animals (Scientific Procedures) Act 1986, under Home Office Licence 70/8389. All experiments were performed following the United Kingdom and European guidelines (Directive 2010/63/UE of the European Parliament and of the Council) and approved by relevant committees. The FLExDUX4 (B6(Cg)-Gt(ROSA) 26Sortm1.1(DUX4*)Plj/J) and HSA-Cre (B6.Cg-Tg(ACTA1-cre/Esr1)2Kesr/J) mice were purchased from the Jackson Laboratory (#028710, #025750) and were crossed to generate the $Cre^{(+/-)}FLExDUX4^{(+/-)}$ mice (named CD/Cre+ and CD/Cre− in the manuscript). *RipK3*-KO mice (C57BL/6 *Ripk3* +/−) were originally kindly provided by Geentech (San Francisco, CA) to generate Mdx/$RipK3^{(-/-)}$ mice and then crossed back to remove the mdx mutation.[25] These three strains were crossed to generate $Cre^{(+/-)}RipK3^{(-/-)}$ and $FLExDUX4^{(+/+)}RipK3^{(-/-)}$ mice and bred together to generate progeny $Cre^{(+/-)}FLExDUX4^{(+/-)}RipK3^{(-/-)}/Cre^{(-/-)}FLExDUX4^{(+/-)}RipK3^{(-/-)}$ (CDR/Cre+ and CDR/Cre−, respectively) used in the experiments. Mice were genotyped as previously described.[26]

Three-week-old animals were weighted three times a week, after weaning. The tamoxifen (MP Biomedicals) injections were realized according to Jones and Jones.[23] Six-week-old mice were injected (IP) with tamoxifen on two consecutive days for a final concentration of 10 mg/kg. Following tamoxifen injection, animals were daily weighed and sacrificed after a week. Muscles were harvested and frozen in liquid nitrogen or liquid-nitrogen-cooled isopentane for further analysis.

Treadmill exhaustion test

The test consisted of an acclimatization period of 5 min on the treadmill (set to an angle of 15°), followed by 5 min at 5 m/min. The speed was then increased by 0.5 m every minute. Electric shock on the treadmill was removed, and mice were encouraged to run by gently pushing them. Mice refusing to run for 10 s were removed from the treadmill, and the total running time was recorded.

Cell culture, viability, cytotoxicity, and caspase activation

Inducible iC2C12-Dux4[10] were cultured in Dulbecco's modified Eagle's medium high glucose with GlutaMAX and no Sodium Pyruvate (Gibco), 20% foetal bovine serum (FBS), and 800 μg/mL G418 (Gibco). For myoblast experiments, iC2C12-Dux4 were seeded into white 96-well plates (3000 cells per well) in growth medium. After 24 h, DUX4 expression was induced by adding doxycycline (Sigma-Aldrich) at a final concentration of 50 to 1000 ng/mL. For myotubes experiments, iC2C12-Dux4 were seeded into white 96-well plates (1500 cells per well) in growth medium. After 48 h, cells were differentiated with Dulbecco's modified Eagle's medium, 2% horse serum, and 10 μg/mL insulin. DUX4 expression was induced after 4 days of differentiation to not disturb myotube formation.[10] Inhibition of apoptosis and/or necroptosis was simultaneously realized to DUX4 induction for 24 h using 20 μM of pan-caspase inhibitor Z-VAD.fmk (Merk Chemicals), 30 μM necrostatin-1, 3 μM GSK872, and 0.2 μM cyclosporin A

DOI: 10.1002/jcsm.12813

(Cambridge Bioscience). Cell survival was determined by CellTiter-Glo luminescent cell viability assay (Promega), membrane permeability by CytoTox-Glo cytotoxicity assay (Promega), and caspase activation by Caspase-Glo 3/7 Assay (Promega) according to the manufacturer's instructions. Luminescence was read by a microplate reader (infinite 200Pro, Tecan, Switzerland).

RNA extraction and quantitative PCR

Total RNAs from cells were extracted using Trizol (Thermo Fisher) according to the manufacturer's protocol. Reverse transcription was performed on 1 μg of total RNA in a 10 μL final volume (Roche Transcriptor First-Strand cDNA Synthesis Kit). Quantitative PCR was designed according to the MIQE standards. Quantitative PCRs were performed on a LightCycler 480 Real-Time PCR System (Roche) in a final volume of 9 μL with 0.2 μL of RT product, 0.4 μM each of forward and reverse primers (Supporting Information, *Table* S1), and 4.5 μL of SYBRGreen Mastermix (Roche).

Fusion index

The fusion index was performed as previously described.[27] Briefly, the cells were plated at 2.4 K/well in 96-well plates. Two days later, proliferation medium was replaced by differentiation medium. The cultures were fixed with 100% EtOH, and MF20 staining was performed (MF20, mouse IgG2b, 1:20 dilution; Developmental Studies Hybridoma Bank). The fusion index was calculated by counting the number of nuclei in MF20-positive myotubes as a percentage of the total number of nuclei.

Histological and immunofluorescence analysis

Histological and immunofluorescence analysis was performed on 10 μm transverse cryosections from the quadriceps muscle. Sections were stained with haematoxylin and eosin, or different Ab. For IgG uptake, the protocol was adapted from Straub *et al*.[28] Sections stored at −80°C were dried at room temperature for 30 min and fixed with 4% paraformaldehyde for 10 min. Following three washes with phosphate buffered saline, staining areas were delimited using a Dako pen. Samples were incubated in 20% FBS, 0.5% Tween 20, 0.5% Triton X100 (except for IgG uptake), and 5% bovine serum albumin. Primary antibodies were diluted in 1% FBS and incubated 2 h at room temperature (IgG uptake analysis) or overnight at 4°C (CD68 positive cells infiltration analysis). Secondary antibodies were diluted in 1% FBS and incubated for 1 h at room temperature, and sections were stained for nuclei with Hoechst for 15 min. For immunofluorescence analysis, rat IgG2A antibody to CD68 (clone FA-11, BioLegend #137001, 1/50), mouse antibody to Laminin (Dako #Z0097, 1/400), goat anti-mouse IgG (Biotin-XX, Invitrogen, 1/400), mouse anti-rat IgG2A eFluor 615 Texas Red (1/400), goat anti-rabbit Alexa Fluor 488 (1/400), and Streptavidin Protein, DyLight 488 (1/400) were used.

Pictures were acquired using ThermoScientific™ Invitrogen™ EVOS™ FL Auto 2 Imaging System and 20× objectives. Sections were entirely scanned, and pictures were analysed using ImageJ software.

Statistical analysis

GraphPad Prism software was used for statistical analyses. Differences between groups were evaluated by either a one-way analysis of variance followed by Dunnett's or Tukey's post hoc tests or a *T*-test as indicated in the figure legends. ****: $P < 0.0001$; ***: $P < 0.001$; **: $P < 0.01$; *: $P < 0.05$.

Results

DUX4 expression causes Ripk1-mediated necroptosis in iC2C12-DUX4 myoblasts

To investigate the role of necroptosis in DUX4 toxicity, we used the iC2C12-DUX4 cells that carry a doxycycline (dox)-inducible DUX4 transgene.[10] In the presence of dox, *DUX4* is expressed in a dose-dependent manner (*Figure* 1A), and consequently, genes downstream of DUX4 are transcribed (*Figures* 1B and S1), and cell viability dramatically decreased (19.3 ± 1.2% of viable cells at 1000 ng/ml of dox) (*Figure* 1C). Non-induced cells expressed low levels of the three major genes involved in necroptosis *Ripk1*, *RipK3*, and *Mlkl*, but after DUX4 induction, expression increased up to 2.52 ± 0.67 times for *Ripk1*, 1.83 ± 0.69 for *Mlkl*, and 3.7 ± 1.34 for *Ripk3* (*Figure* 1D–1F, respectively).

We next asked whether increased necroptosis gene levels have any effect on cell viability. First, we investigated the role of the caspases by cultivating the iC2C12-DUX4 cells in the presence of 200 ng/mL of dox (dose leading to an important expression of *DUX4* with a cell viability of 35%; *Figure* 1A and 1C) and with different doses of Z-VAD, a pan-caspase inhibitor. No change in cell survival was observed with and without Z-VAD (*Figure* 2A), indicating that caspases are not involved in the death of the iC2C12-DUX4 cells. It is worth noting that the addition of Z-VAD induced a non-specific increase of cell survival that is due to the presence of DMSO (*Figure* S2A). We confirmed that caspase 3/7 activity increased after DUX4 expression and was correctly inhibited in the presence of Z-VAD (*Figure* S2B). We next investigated the role of necroptosis in the DUX4-mediated cell death by the addition

DOI: 10.1002/jcsm.12813

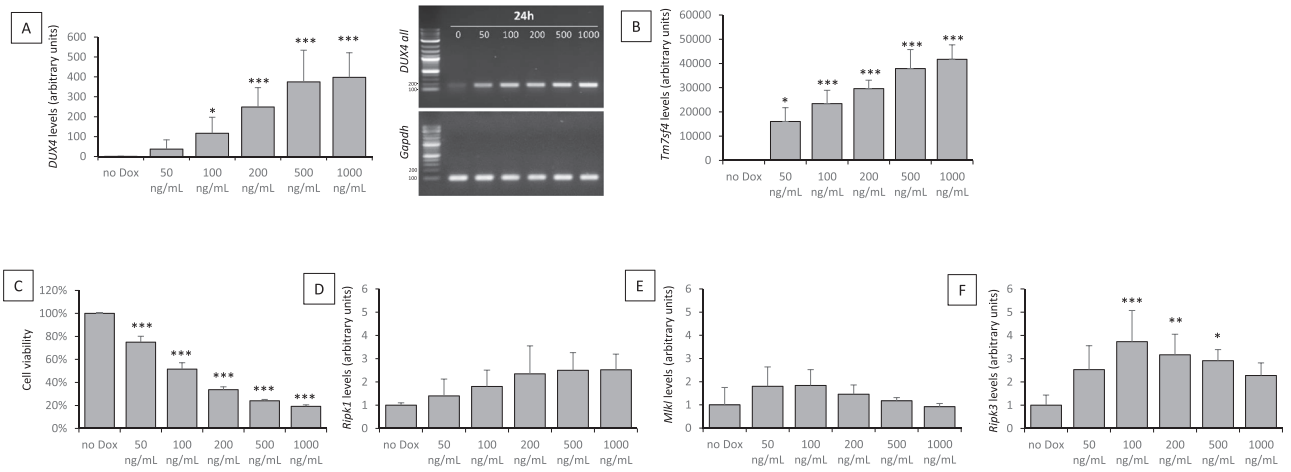

Figure 1 DUX4 expression triggers cell death in iC2C12-DUX4 myoblasts. *(A, B, D–F)* Expression of *DUX4*, *Tm7sf4*, *Ripk1*, *Mlkl*, or *Ripk3*, respectively (RT-qPCR) 24 h after addition of different concentration of dox in iC2C12-DUX4 myoblasts. *(C)* Cell viability assay [adenosine triphosphate (ATP) assay] at 24 h after dox induction at various concentrations. Data represent the mean ± standard deviation on three independent experiments; ****: $P < 0.0001$; ***: $P < 0.001$; **: $P < 0.01$; *: $P < 0.05$ by one-way analysis of variance with Dunnett's post hoc test.

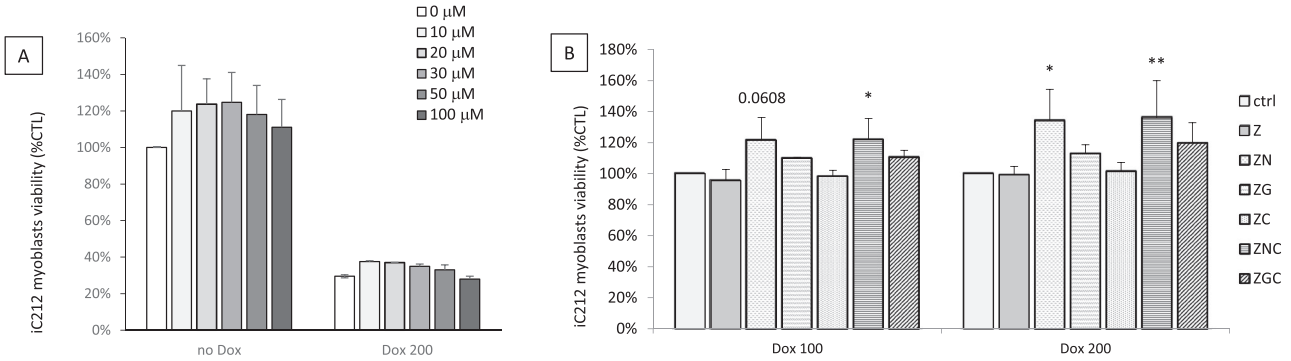

Figure 2 Necroptosis participates in DUX4-mediated cell death. *(A)* Cell viability on iC2C12-DUX4 myoblasts at 48 h of induction without or with dox (200 ng/mL) and treatment with various concentrations of the pan-caspase inhibitor Z-VAD. *(B)* ATP assay on iC2C12-DUX4 myoblasts at 48 h of induction with 100 or 200 ng/mL of dox and treatment with different molecules (Z: ZVAD 20 μM, N: necrostatin-1 30 μM; G: GSK'872 2 μM; C: cyclosporin A 0.2 μM) alone or in combination. Data are presented as means ± standard deviation; *: $P < 0.05$ by one-way analysis of variance with Dunnett's post hoc test.

of either necrostatin-1 (RIPK1 inhibitor) or GSK'872 (RIPK3 inhibitor) alone or in combination. The iC2C12-DUX4 viability was assessed for two different doses of dox, and the results are expressed as the percentage of cells alive in the presence of the different compounds compared with the condition without them. Z-VAD was always added to eliminate any bias linked to caspases 3/7 activation/synergic effect. The only condition that induced a cell rescue was when necrostatin-1 was present. In the presence of 100 ng/mL of dox, the two combinations Z-VAD/necrostatin-1 and Z-VAD/necrostatin-1/cyclosporine A lead to an increase of cell survival by 22 ± 15% ($P = 0.06$; *Figure* 2B). Similar results were obtained when the dox concentration was 200 ng/mL (increase of cells survival by 34 ± 20%, $P = 0.011$ when necrostatin-1 is present), thus demonstrating the role of Ripk1-mediated necroptosis in DUX4-mediated cell death in iC2C12-DUX4 myoblasts.

DUX4 expression causes RIPK3-mediated necroptosis in iC2C12-DUX4 myotubes

We next investigated DUX4-mediated toxicity in iC2C12-DUX4 myotubes. An MF20 staining was realized to assess myotube formation, and we calculated that the fusion index was 20.3% (*Figure* S3). We observed an increase of *DUX4* mRNA after addition of dox in a dose-dependent manner (*Figure* 3A), associated with an increase of several genes downstream of DUX4 including *Tm7sf4* (*Figure* 3B), *Wfdc3*, *Duxbl*, and *Snx30* (*Figure* S4) and a decrease in cell viability (*Figure* 3C). The expression

DOI: 10.1002/jcsm.12813

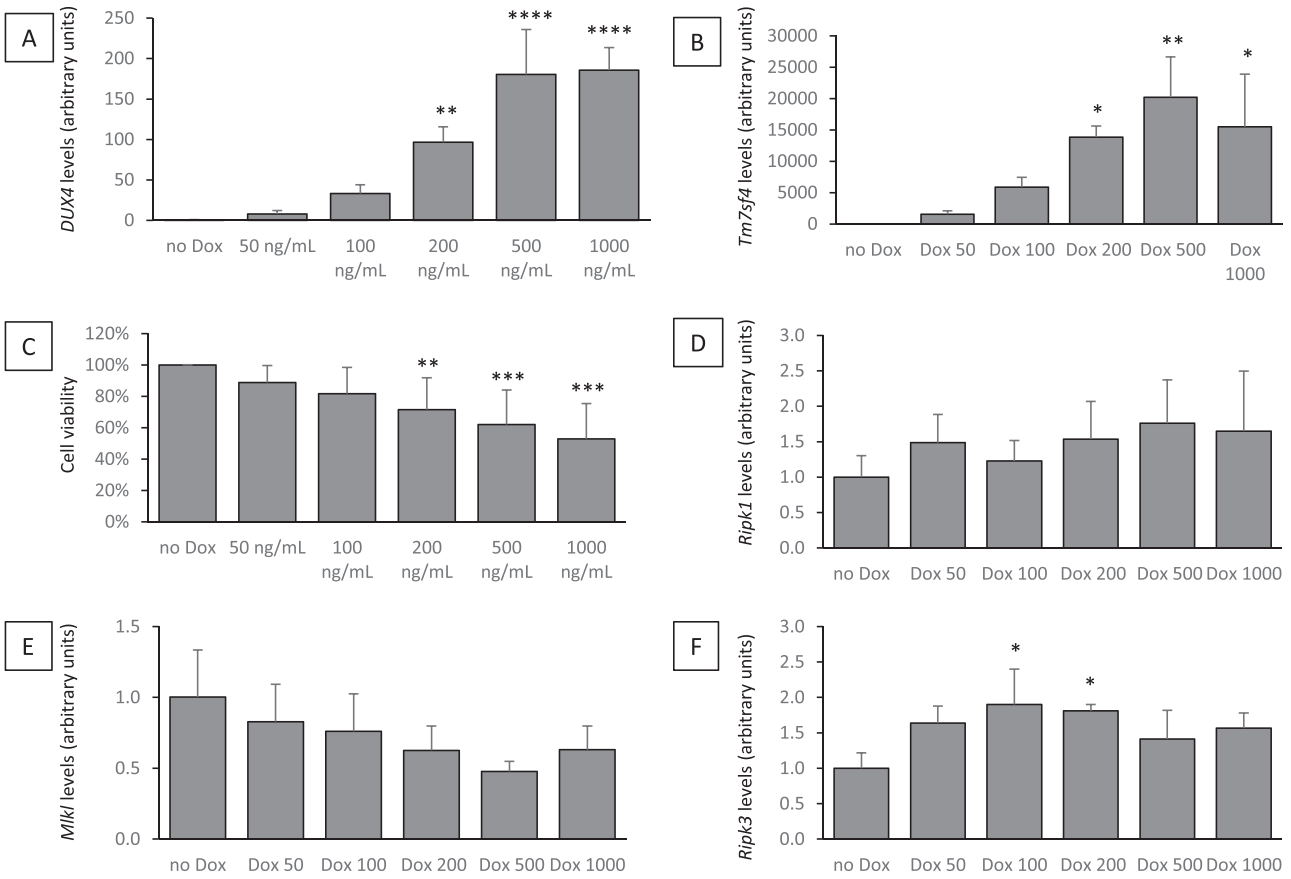

Figure 3 DUX4 expression triggers cell death in iC2C12-DUX4 myotubes. *(A, B, D–F)* Expression of *DUX4*, *Tm7sf4*, *Ripk1*, *Mlkl*, or *Ripk3*, respectively (RT-qPCR) 24 h after addition of different concentration of dox in iC2C12-DUX4 myotubes after 4 days of differentiation. *(C)* Cell viability assay [adenosine triphosphate (ATP) assay] at 24 h after dox induction at various concentrations. Data represent the mean ± standard deviation on three independent experiments; ****: $P < 0.0001$; ***: $P < 0.001$; **: $P < 0.01$; *: $P < 0.05$ by one-way analysis of variance with Dunnett's post hoc test.

of *Ripk1* and *Mlkl* was not affected by DUX4 expression (*Figure* 3D and 3E). *Ripk3* level was increased up to 1.9 ± 0.5-fold (*Figure* 3F).

We next analysed the effects of the different inhibitors on iC2C12-DUX4 myotubes. Again, the results are expressed as the percentage of live cells in the presence of the different compounds compared with the control condition without. We observed no effect of Z-VAD arguing against a major role of caspases in DUX4-mediated toxicity (*Figure* 4A). When the cells were cultivated with necrostatin-1 in the presence of dox (1000 ng/mL), necrostatin-1 concentrations above 60 μM conferred a good protection against cell death (up to 60 ± 6% of viable cells in the presence of 60 μM necrostatin-1 compared with 39 ± 1% without, $P < 0.0001$; *Figure* 4A), necrostatin-1 concentrations of 150 or 300 μM leading to up to 85 ± 2% viable cells (*Figure* 4A). When the iC2C12-DUX4 myotubes were incubated with GSK'872, a massive cell death rescue was observed at low concentrations (up to 67 ± 2% of viable cells in the presence of 3 μM GSK'872 compared with 39 ± 1% without, $P < 0.0001$; *Figure* 4A). Higher GSK'872 concentrations slightly improved cell viability (up to 77 ± 4% of viable cells in the presence of 6 μM GSK'872, $P < 0.0001$; *Figure* 4A). These results demonstrated the role of necroptosis in DUX4-mediated myotube death. The different compounds were next added separately or together to iC2C12-DUX4 myotubes that were incubated with dox (1000 ng/mL). No modification of the cell viability was observed in the presence of 20 μM Z-VAD/30 μM necrostatin-1, but when necrostatin-1 concentration was increased to 90 μM (N+), the combination 20 μM Z-VAD/90 μM necrostatin-1 leads to cell rescue (increase of cell survival by 54 ± 20% with necrostatin-1 compared with 10 ± 10% for Z-VAD alone). The best cell rescue was observed in the presence of GSK'872. Indeed, at low (2 μM, G) or high (4 μM, G+) concentration, GSK'872 increased cell viability by 2.1-fold (*Figure* 4B). The combination necrostastin-1/GSK'872 did not show any additive or synergistic effect. These results demonstrated the important role of necroptosis in DUX4-mediated cell death. RIPK3, but also to a lesser extent RIPK1, participated in DUX4-mediated cell toxicity.

DOI: 10.1002/jcsm.12813

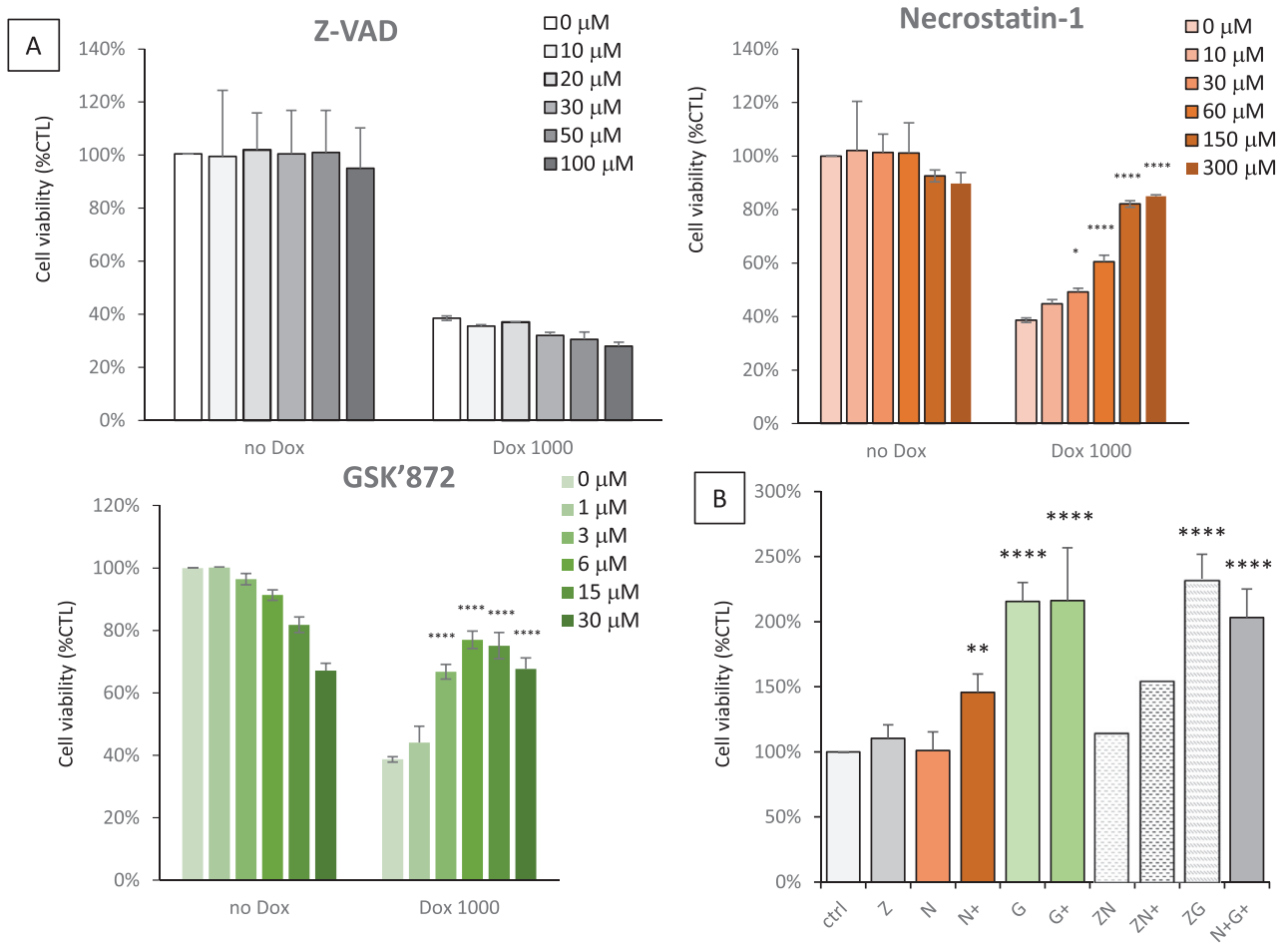

Figure 4 Ripk3 inhibition decreased DUX4-mediated cell death in iC2C12-DUX4 myotubes. *(A)* iC2C12-DUX4 viability in the presence of dox 1000 ng/mL and treated with different doses of Z-VAD, necrostatin-1, or GSK'872. *(B)* Cell viability in the presence of dox 1000 ng/mL with the different compounds alone or in combination. Z: Z-VAD (20 µM), N: necrostatin-1 (30 µM), N+: necrostatin-1 (90 µM), G: GSK'872 (2 µM); G+: GSK'872 (4 µM). Data are presented as means ± standard deviation; ****: $P < 0.0001$; ***: $P < 0.001$; **: $P < 0.01$; *: $P < 0.05$ by one-way analysis of variance with Dunnett's post hoc test.

Necroptosis participates in DUX4-mediated toxicity in vivo

The experiments performed in cell culture suggested that necroptosis is a key element of DUX4-mediated toxicity. To evaluate the role of necroptosis *in vivo*, we used the cre-inducible DUX4 transgenic mouse model (FLExDUX4, here called CD) that conditionally expresses human DUX4 following tamoxifen injection.[23] We crossed this model with a Ripk3-deficient mouse model,[24] leading to the new transgenic CDR (*DUX4*−/+*Ripk3*−/−*Cre*-positive or -negative) mouse model (*Figure* S5). After tamoxifen injection, total body weight was measured, and *Figure* 5A represents the variation of the total body weight gain (in percentage) from the beginning of treatment to animal death. In CD- and CDR-cre-negative animals, a 13–15% increase of the total body weight was observed (*Figure* 5A), but in both CD- and CDR-cre-positive animals, a decrease of the total body weight was noted. This decrease is less pronounced in the CDR animals (in males, 91.4 ± 3.9% for the CDR/Cre+ and 84.6 ± 4.8% for the CD/Cre+, $P = 0.02$; in females, 90.8 ± 6.7% for the CDR/Cre+ and 82.5 ± 4.9% for the CD/Cre+, $P = 0.1$). These results indicate the role of necroptosis in DUX4-mediated toxicity leading to weight loss. We also performed a treadmill exhaustion test on both the CDR/cre + and CD/Cre+ males (*Figure* 5B), which revealed that the CDR-cre+ animals were able to run four times longer than the Ripk3-competent animals ($P = 0.055$).

We next analysed the weights of the tibialis anterior (TA) and quadriceps (QUA). CD- and CDR-Cre-negative animals showed similar TA or QUA muscle weights (*Figure* 5C and 5D); CD- and CDR-Cre-positive animals showed also comparable weights of the TA (~25 mg for the males and ~20–22 mg for the females). However, QUA weights were higher in CDR-

DOI: 10.1002/jcsm.12813

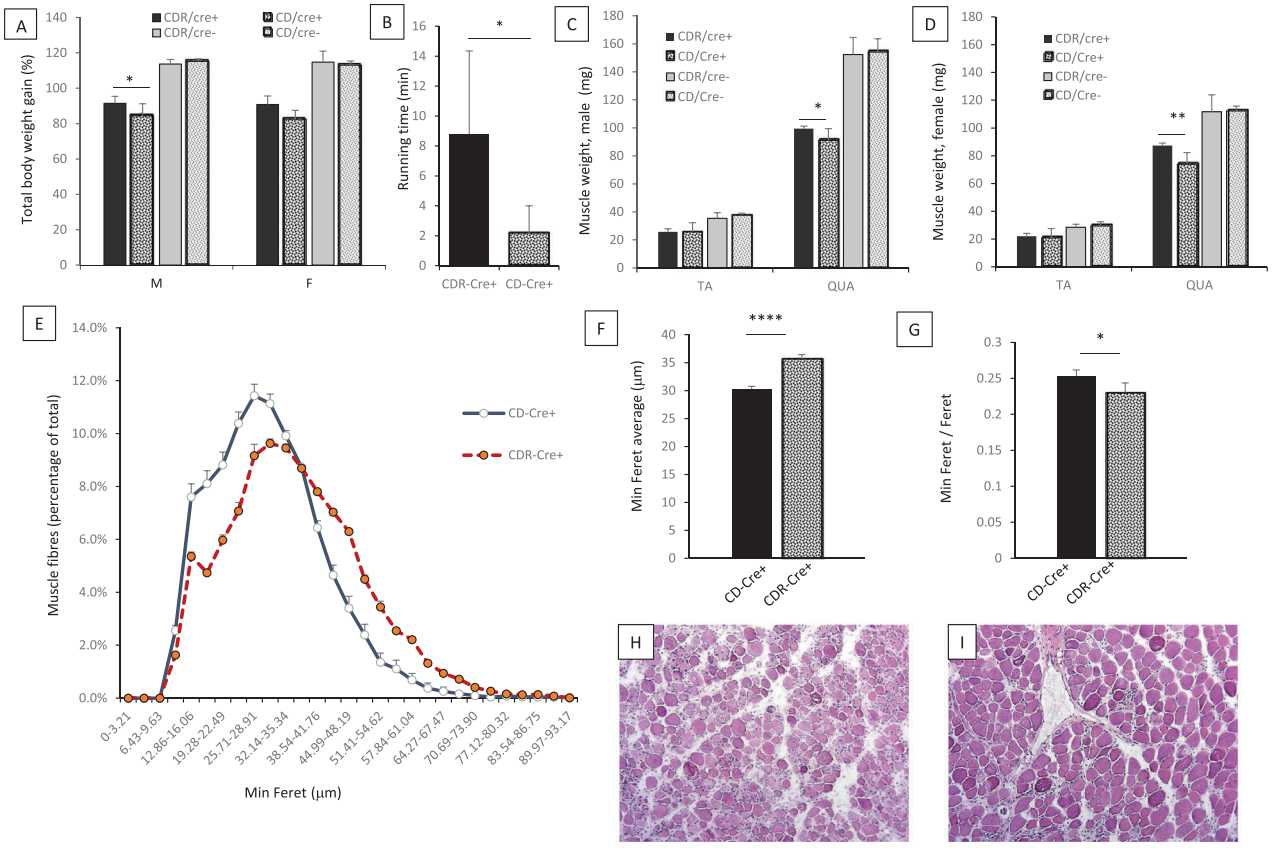

Figure 5 *In vivo* DUX4-mediated toxicity leading to weight loss is triggered by Ripk3. *(A)* Variation of the total body weight gain (in percentage) from the beginning of treatment to animal death. *(B)* Total running time was measured on a 15° angled treadmill system. *(C* and *D)* Weights of the tibialis anterior (TA) and quadriceps (QUA) in the different models. *N* = 4–8 animals per group. Male *(C)* or female *(D)*. Six-week-old animals were given a 2 day treatment of 10 mg/kg tamoxifen delivered intraperitoneally, and the mice were killed 5 days after the last injection. CD: DUX4−/+ animals; CDR: DUX4−/+Ripk3−/−. Data are presented as means ± standard deviation; ****: $P < 0.0001$; **: $P < 0.01$; *: $P < 0.05$ by one-way analysis of variance with Dunnett's post hoc test. *(E)* The quadriceps muscles (female only) were sectioned and labelled with laminin, and the min Feret was calculated for each muscle fibre. *(F* and *G)* The min Feret average *(F)* and the ratio min Feret/Feret were calculated in the quadriceps of CD- and CDR-Cre+ females. *(H* and *I)* Haematoxylin and eosin staining of CD-Cre+ *(H)* and CDR-Cre+ *(I)* muscle cross sections.

Cre-positive than in CD-Cre-positive animals (in males, 99.4 mg ± 6.6 for the CDR/Cre+ and 90.9 mg ± 8.4 for the CD/Cre+, $P = 0.02$; in females, 87.3 mg ± 6.2 for the CDR/Cre+ and 73.8 mg ± 6 for the CD/Cre+, $P = 0.006$), showing that QUA weights are higher when RIPK3 is not expressed.

We examined morphological and physiological aspects of the QUA only because variation in muscle weight was not observed in the TA of mice expressing or not RIPK3. The measure of the minimal Feret's diameter revealed the presence of smaller fibres in the CD/Cre+ than in the CDR/Cre+ mice (*Figure* 5E and 5F), which is in accordance with the reduced muscle weight in the Ripk3-competent animals. We also calculated the min Feret/Feret ratio to analyse fibre circularity (*Figure* 5G). This ratio was higher in the CD/Cre+ group ($P = 0.017$), showing a lower loss of the normal polygonal myofibre shape in the Ripk3-deficient animals. The roundness of the fibres was clearly visible on standard histological staining with haematoxylin and eosin, which revealed major histological changes in both CD/Cre+ and CDR/Cre+ animals (*Figure* 5H and 5I, respectively) with signs of myopathy (inflammation, degenerative fibres). However, these signs were less pronounced in the CDR/Cre+ than in the CD/Cre+ mice.

Next, we investigated the expression of *Ripk3*, *Ripk1*, and *Mlkl* in the QUA. As expected, no expression of *Ripk3* was observed in the Ripk3-deficient mice (CDR-cre-positive or –negative; *Figure* 6). Expression of *Ripk1*, *Ripk3*, and *Mlkl* was higher in the CD-cre+ animals compared with the CD-Cre-negative mice (5.2-fold, 3.1-fold, and 2.9-fold for *Ripk1*, *Ripk3*, and *Mlkl*, respectively; $P < 0.0001$, 0.002, and 0.005, respectively), thus showing that DUX4 expression induces necroptosis network activation. Interestingly, in the presence of Cre, the absence of *Ripk3* did not modify or only slightly modify the global mRNA levels of *Ripk1* and *Mlkl* (CDR/Cre+ vs. CD/Cre+; *Figure* 6). However, the expression levels of two genes downstream of DUX4 were reduced in the CDR/Cre+ compared with the CD/Cre+ animals: by 3.1-fold ($P = 0.02$) and 2.1-fold ($P = 0.0005$) for *Tm7sf4* and *mDuxbl*, respectively. Expression levels of *Wfdc3* remained

DOI: 10.1002/jcsm.12813

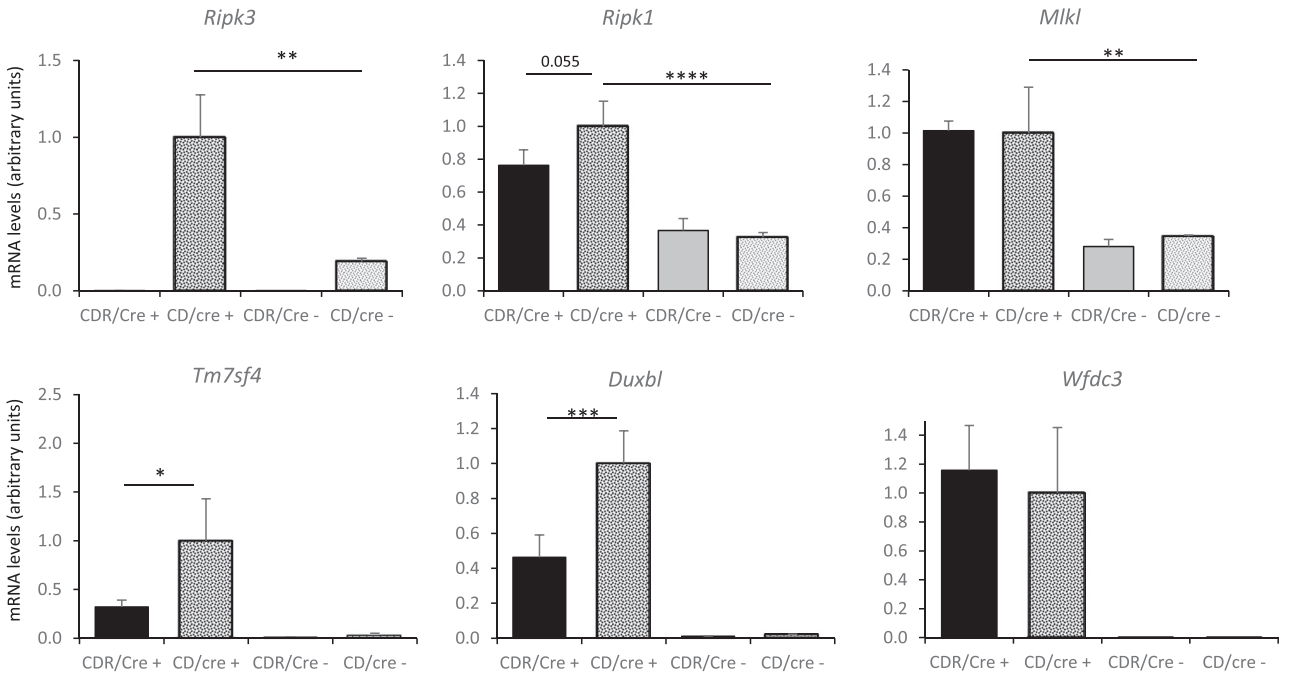

Figure 6 Expression of necroptotic and DUX4-network genes in the CD mice. *Ripk3*, *Ripk1*, and *Mlkl* and *Tm7sf4*, *Duxbl*, and *Wfdc3* were measured in the quadriceps. Six-week-old female mice were given a 2 day treatment of 10 mg/kg tamoxifen delivered intraperitoneally, and the mice were killed 5 days after the last injection. N = 2 to 5 muscles per group. CD: DUX4−/+ animals; CDR: DUX4−/+Ripk3−/−. Data are presented as means ± standard deviation; ****: $P < 0.0001$; ***: $P < 0.001$; **: $P < 0.01$; *: $P < 0.05$ by one-way analysis of variance with Tukey's post hoc test.

unchanged. As expected, in the absence of Cre, genes downstream of DUX4 are not expressed.

RIPK3 deficiency ameliorates muscle phenotype of DUX4-expressing mice

We next questioned whether *Ripk3* depletion ameliorates muscle phenotype after DUX4 expression. We investigated the presence of an inflammatory response and measured the muscle area infiltrated by macrophages using a CD68 antibody. *Ripk3*−/− CD mice (CDR) had over seven-fold decrease (P = 0.039) compared with RIPK3-competent CD mice (*Figure* 7A), indicating a role of RIPK3 in inflammatory response to DUX4 expression. Myonecrosis was also investigated by IgG uptake labelling. The percentage of IgG-positive area was four-fold decreased in CDR mice (P = 0.007) (*Figure* 7B). Finally, we measured the percentage of nuclear DNA fragmentation in both the CD and CDR quadriceps muscles. We observed 30 ± 9% of fragmented nuclei in the Ripk3-negative animals compared with 40 ± 8% in the Ripk3-competent animals (*Figure* S6), which is not statistically different (P = 0.18, T-test). This result shows that inhibition of necroptosis is not accompanied by a modification of the number of apoptotic nuclei. RIPK3 deficiency reduces inflammation-mediated muscle damage and ameliorates the muscle phenotype of DUX4-expressing mice, which demonstrates the role of necroptosis in DUX4-mediated toxicity.

Discussion

These studies demonstrate the involvement of the necroptosis pathway in the DUX4-mediated cells death. Necroptosis is a cellular response to a stress that can be caused by several triggers including inflammation, and muscle inflammation has been reported in up to 1/3 of skeletal muscle FSHD biopsies.[29] Transient expression of DUX4 was previously shown to induce many genes involved in inflammation.[30] However, it was recently proposed that cell death may not be the consequence of inflammation but rather its cause, and cell death may precede or trigger the inflammatory response.[31] Further studies are required to determine to what extent cell death triggers or causes inflammation in DUX4-expressing cells/muscles.

Previously, a possible pro-apoptotic role of DUX4 was proposed, based on (i) a caspase 3/7 activity found after DUX4 overexpression *in vitro*,[10,32] (ii) the presence of TUNEL-positive nuclei in Xenopus embryos overexpressing DUX4,[33] (iii) the activation of a p53-dependent cell death observed after DUX4 overexpression in mouse muscles and p53-knockout mouse background suppressed AAV-DUX4 toxicity,[13] (iv) the decrease of caspase 3/7 activation after treatment of FSHD myotubes with p53 pathway inhibitors,[12] and (v) bio-informatics analysis.[11,18,34] DUX4-expressing cells have been also described to be more susceptible to oxidative stress-induced death.[10,35–37] However, the role of p53 in

DOI: 10.1002/jcsm.12813

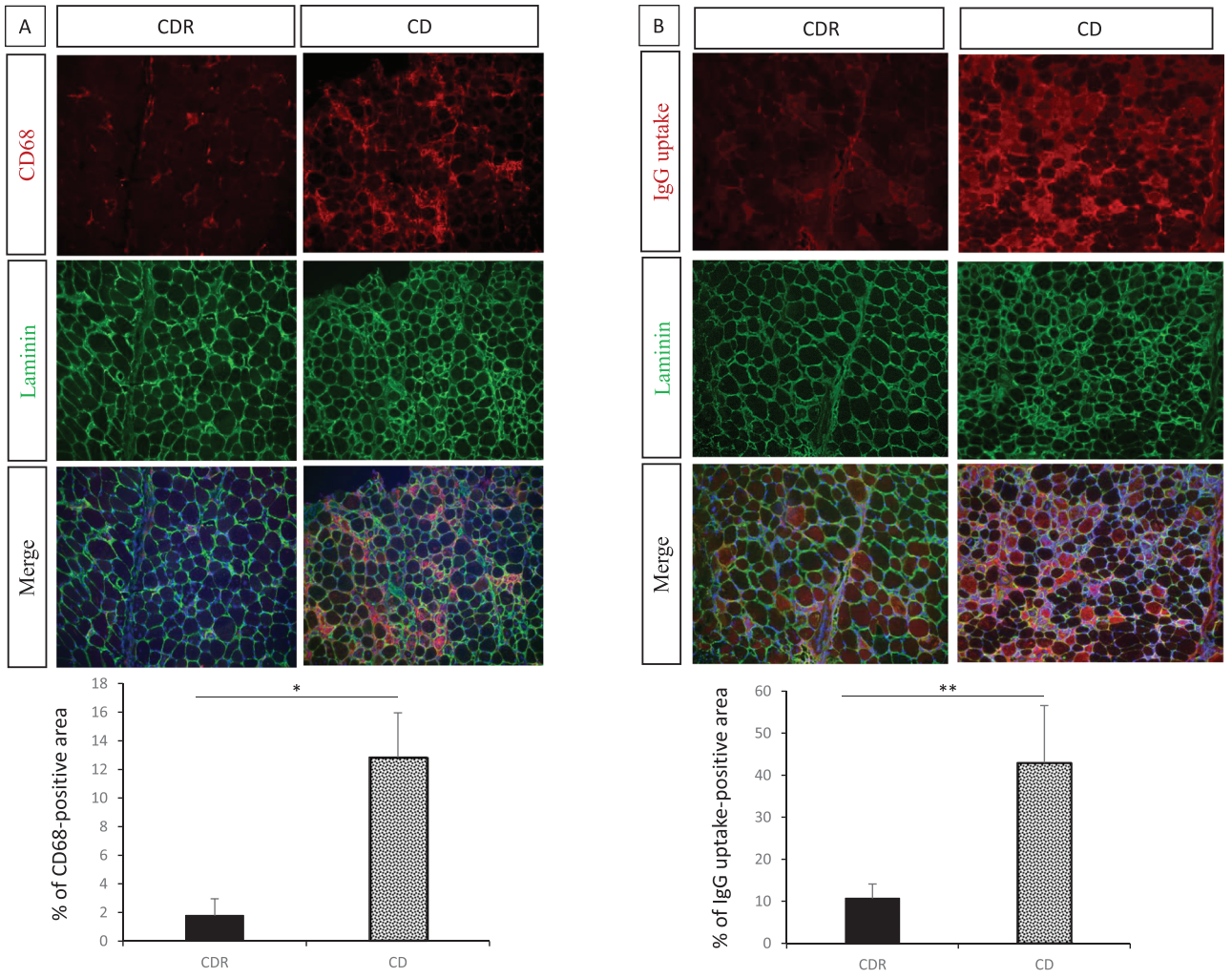

Figure 7 Ripk3 deficiency ameliorates muscle phenotype in mouse. Representative images of transversed sections of mouse quadriceps labelled with Laminin and CD68 *(A)* or Laminin and IgG uptake *(B)*. Quantification of CD68- *(C)* or IgG-uptake- *(D)* positive areas. Scale bar 200 μm. Data represent the mean ± standard error of the mean on three to five animals per group. CD: DUX4−/+ animals; CDR: DUX4−/+Ripk3−/−. The Student's *T*-test was performed. $*P < 0.05$.

DUX4 toxicity is under debate, and recent experiments have shown that p53 genes do not respond to DUX4 expression and p53 status does not impact DUX4-mediated death both *in vitro* and *in vivo*.[15] Moreover, the addition of antioxidant to the cells decreased DUX4 toxicity rather than rescued them,[10] and supplementation with antioxidants in FSHD patients improved only very slightly the maximum voluntary contraction and endurance of the quadriceps muscles.[38]

Here, we clearly demonstrated that DUX4 mediates a necroptosis-dependent cell death. *In vitro*, the addition of the Z-VAD pan-caspase inhibitor to the iC2C12-DUX4 myotubes did not increase cell survival, suggesting a limited role of apoptosis in myotube death. The involvement of necroptosis was established by the addition of the GSK'872 RIPK3 inhibitor (in combination with Z-VAD) that leads to a two-fold increase of the number of viable cells. Interestingly, in iC2C12 myoblasts, Ripk1 is the main regulator of necroptosis pathway as a 20% increase of viable cells is observed in the presence of necrostatin-1. Ripk3 is also involved because there is 10% more viable cells in the presence of GSK'872. Again, our data suggest that apoptosis does not participate in cell death and the addition Z-VAD did not modify the percentage of viable cells. This shows that cell death mechanisms are different in myoblasts and myotubes and results obtained on myoblasts cannot be extrapolated to myotubes and even less to mature muscle fibres.

In vivo, we created a new transgenic and viable mouse model lacking Ripk3 and expressing DUX4 only after tamoxifen injection. We chose to target Ripk3 because Ripk1-deficient mice show perinatal lethality.[39] We observed that *Ripk3* deficiency reduces the weight loss observed after DUX4 expression but does not rescue it. This demonstrated the involvement of *Ripk3 in vivo* and suggested

DOI: 10.1002/jcsm.12813

that Ripk3-independent pathways are also responsible for cell death.

The next step is to evaluate the involvement of necroptosis in FSHD patients. In one hand, the necroptosis pathway has been described to play a role in the pathogenesis of various pathologies across the body including pulmonary, cardiovascular, renal, hepatic, or neurologic systems (for review, see previous works[20,40]). But in the other hand, regulated cell death, including necroptosis, preserves organ homeostasis by removing the cells that have been damaged beyond recovery. Regulated cell death is activated when the cells fail to repair damage and restore cellular homeostasis. In the case of DUX4 expression, one can imagine that the cascade of misregulated genes leads to the activation of necroptosis and to cell death eventually, as suggested by our experiments in the iC2C12 cells. However, in the iC2C12 cells, each cell carries the DUX4 gene, which can be activated upon doxycycline addition, leading to a relatively high expression of DUX4. In FSHD muscle, DUX4 expression occurs in burst and a lower expression is expected, which is in agreement with the slow disease progression observed in FSHD patients. This difference in *DUX4* levels in cells and muscle biopsies could lead to different cell mechanisms and needs to be experimentally validated. These results open new avenues of research for skeletal muscle diseases and for FSHD in particular.

Acknowledgements

We thank Michael Kyba for the iC2C12 cells and Peter Jones for the FLeXDUX4 mouse model. We thank Dr V.M. Dixit for the Ripk3 knockout mice. The authors of this manuscript certify that they comply with the ethical guidelines for authorship and publishing in the *Journal of Cachexia, Sarcopenia and Muscle*.[41]

Conflict of interest

M.B., V.M. and J.D. are named inventors of a patent entitled 'Therapeutic treatments for FSHD' that has been filled by UCL. The other authors have declared that no conflict of interest exists.

Funding

This study was funded by the FSH Society Grant FSHS-22017-7. M.B. is supported by: Association Française contre les Myopathies (AFM) via TRANSLAMUSCLE (PROJECT 19507 and 22946). All research at Great Ormond Street Hospital NHS Foundation Trust and UCL Great Ormond Street Institute of Child Health is made possible by the NIHR Great Ormond Street Hospital Biomedical Research Centre. The views expressed are those of the author(s) and not necessarily those of the NHS, the NIHR, or the Department of Health.

Online supplementary material

Additional supporting information may be found online in the Supporting Information section at the end of the article.

Figure S1. Expression of Wfdc3, Duxbl and Snx30 after addition different concentration of Dox in iC2C12-DUX4 myoblasts. Data represents the mean ± SD on 3 independent experiments and are presented as means ± SD; ****: $P < 0.0001$; ***: $p < 0.001$; **: $p < 0.01$; *: $p < 0.05$ by one-way ANOVA with Dunnett's post hoc test

Figure S2. (A) The presence of DMSO induced a non-specific increase of cell survival. (B) Caspase 3/7 activity increased after DUX4 expression and is correctly inhibited in the presence of Z-VAD

Figure S3. MF20 staining on iC2C12 cells after 4 days of differentiation. At Day 4 of differentiation, cells were stained with MF20 antibody recognizing all the myosin heavy chain and counterstained with 40,6-diamidino-2-phenylindole. Fusion index was calculated as described in Krom et al. 2012. Fusion index was 20.3%. Scale bar: 200 mm

Figure S4. Several DUX4 downstream genes (Wfdc3, Duxbl and Snx30) are increased in a dose dependent manner after addition of Dox in iC2C12-DUX4 myotubes. Data represents the mean ± SD on 3 independent experiments and are presented as means ± SEM; ****: $P < 0.0001$; ***: $p < 0.001$; **: $p < 0.01$; *: $p < 0.05$ by one-way ANOVA with Dunnett's post hoc test

Figure S5. creation of the new transgenic CDR (DUX4−/+Rip−/−) cre-negative or –positive mouse model

Figure S6. quadriceps sections were labelled for DNA fragmentation using the TACS•XL®-DAB In Situ Apoptosis Detection Kit (Trevigen), according to the manufacturer instructions. At least 2000 nuclei were analyzed per section. Data represents the mean ± SEM on 3–5 animals/group. CD: DUX4−/+ animals; CDR: DUX4−/+Ripk3−/−. Student T-Test was performed. $P > 0.5$.

Table S1. Supporting Information

References

1. Van Deutekom JC, Wijmenga C, Van Tienhoven EA, Gruter AM, Hewitt JE, Padberg GW, et al. FSHD associated DNA rearrangements are due to deletions of integral copies of a 3.2 kb tandemly repeated unit. *Hum Mol Genet* 1993;**2**:2037–2042.
2. Wijmenga C, Hewitt JE, Sandkuijl LA, Clark LN, Wright TJ, Dauwerse HG, et al. Chromosome 4q DNA rearrangements associated with facioscapulohumeral muscular dystrophy. *Nat Genet* 1992;**2**:26–30.
3. Lemmers RJ, Tawil R, Petek LM, Balog J, Block GJ, Santen GW, et al. Digenic inheritance of an SMCHD1 mutation and an FSHD-permissive D4Z4 allele causes facioscapulohumeral muscular dystrophy type 2. *Nat Genet* 2012;**44**:1370–1374.
4. Snider L, Asawachaicharn A, Tyler AE, Geng LN, Petek LM, Maves L, et al. RNA transcripts, miRNA-sized fragments and proteins produced from D4Z4 units: new candidates for the pathophysiology of facioscapulohumeral dystrophy. *Hum Mol Genet* 2009;**18**:2414–2430.
5. Ferreboeuf M, Mariot V, Furling D, Butler-Browne G, Mouly V, Dumonceaux J. Nuclear protein spreading: implication for pathophysiology of neuromuscular diseases. *Hum Mol Genet* 2014;**23**:4125–4133.
6. Snider L, Geng LN, Lemmers RJ, Kyba M, Ware CB, Nelson AM, et al. Facioscapulohumeral dystrophy: incomplete suppression of a retrotransposed gene. *PLoS Genet* 2010;**6**:e1001181.
7. Broucqsault N, Morere J, Gaillard MC, Dumonceaux J, Torrents J, Salort-Campana E, et al. Dysregulation of 4q35- and muscle-specific genes in fetuses with a short D4Z4 array linked to Facio-Scapulo-Humeral Dystrophy. *Hum Mol Genet* 2013;**22**:4206–4214.
8. Ferreboeuf M, Mariot V, Bessieres B, Vasiljevic A, Attie-Bitach T, Collardeau S, et al. DUX4 and DUX4 downstream target genes are expressed in fetal FSHD muscles. *Hum Mol Genet* 2014;**23**:171–181.
9. DeSimone AM, Pakula A, Lek A, Emerson CP Jr. Facioscapulohumeral muscular dystrophy. *Compr Physiol* 2017;**7**:1229–1279.
10. Bosnakovski D, Xu Z, Gang EJ, Galindo CL, Liu M, Simsek T, et al. An isogenetic myoblast expression screen identifies DUX4-mediated FSHD-associated molecular pathologies. *EMBO J* 2008;**27**:2766–2779.
11. Rickard AM, Petek LM, Miller DG. Endogenous DUX4 expression in FSHD myotubes is sufficient to cause cell death and disrupts RNA splicing and cell migration pathways. *Hum Mol Genet* 2015;**24**:5901–5914.
12. Block GJ, Narayanan D, Amell AM, Petek LM, Davidson KC, Bird TD, et al. Wnt/beta-catenin signaling suppresses DUX4 expression and prevents apoptosis of FSHD muscle cells. *Hum Mol Genet* 2013;**22**:390–396.
13. Wallace LM, Garwick SE, Mei W, Belayew A, Coppee F, Ladner KJ, et al. DUX4, a candidate gene for facioscapulohumeral muscular dystrophy, causes p53-dependent myopathy in vivo. *Ann Neurol* 2011;**69**:540–552.
14. Dandapat A, Bosnakovski D, Hartweck L, Arpke R, Baltgalvis K, Vang D, et al. Dominant lethal pathologies in male mice engineered to contain an X-linked DUX4 transgene. *Cell Rep* 2014;**8**:1484–1496, Epub 2014 Aug 28.
15. Bosnakovski D, Gearhart MD, Toso EA, Recht OO, Cucak A, Jain AK, et al. p53-independent DUX4 pathology in cell and animal models of facioscapulohumeral muscular dystrophy. *Dis Model Mech* 2017;**10**:1211–1216.
16. DeSimone AM, Leszyk J, Wagner K, Emerson CP Jr. Identification of the hyaluronic acid pathway as a therapeutic target for facioscapulohumeral muscular dystrophy. *Sci Adv* 2019;**5**:eaaw7099.
17. Bosnakovski D, Da Silva MT, Sunny ST, Ener ET, Toso EA, Yuan C, et al. A novel P300 inhibitor reverses DUX4-mediated global histone H3 hyperacetylation, target gene expression, and cell death. *Sci Adv* 2019;**5**:eaaw7781.
18. Lek A, Zhang Y, Woodman KG, Huang S, DeSimone AM, Cohen J, et al. Applying genome-wide CRISPR-Cas9 screens for therapeutic discovery in facioscapulohumeral muscular dystrophy. *Sci Transl Med*. 2020;**12**(536):eaay0271. https://doi.org/10.1126/scitranslmed.aay0271
19. Vanden Berghe T, Linkermann A, Jouan-Lanhouet S, Walczak H, Vandenabeele P. Regulated necrosis: the expanding network of non-apoptotic cell death pathways. *Nat Rev Mol Cell Biol* 2014;**15**:135–147.
20. Khoury MK, Gupta K, Franco SR, Liu B. Necroptosis in the pathophysiology of disease. *Am J Pathol* 2020;**190**:272–285.
21. Mcquade T, Cho Y, Chan FK. Positive and negative phosphorylation regulates RIP1- and RIP3-induced programmed necrosis. *Biochem J* 2013;**456**:409–415.
22. Silke J, Rickard JA, Gerlic M. The diverse role of RIP kinases in necroptosis and inflammation. *Nat Immunol* 2015;**16**:689–697.
23. Jones T, Jones PL. A cre-inducible DUX4 transgenic mouse model for investigating facioscapulohumeral muscular dystrophy. *PLoS ONE* 2018;**13**:e0192657.
24. Newton K, Sun X, Dixit VM. Kinase RIP3 is dispensable for normal NF-κBs, signaling by the B-cell and T-cell receptors, tumor necrosis factor receptor 1, and Toll-like receptors 2 and 4. *Mol Cell Biol* 2004;**24**:1464–1469.
25. Morgan JE, Prola A, Mariot V, Pini V, Meng J, Hourde C, et al. Necroptosis mediates myofibre death in dystrophin-deficient mice. *Nat Commun* 2018;**9**:3655.
26. Joubert R, Mariot V, Dumonceaux J. One-hour universal protocol for mouse genotyping. *Muscle Nerve* 2020;**61**:801–807.
27. Krom YD, Dumonceaux J, Mamchaoui K, Den Hamer B, Mariot V, Negroni E, et al. Generation of isogenic D4Z4 contracted and noncontracted immortal muscle cell clones from a mosaic patient: a cellular model for FSHD. *Am J Pathol* 2012;**181**:1387–1401.
28. Straub V, Rafael JA, Chamberlain JS, Campbell KP. Animal models for muscular dystrophy show different patterns of sarcolemmal disruption. *J Cell Biol* 1997;**139**:375–385.
29. Arahata K, Ishihara T, Fukunaga H, Orimo S, Lee JH, Goto K, et al. Inflammatory response in facioscapulohumeral muscular dystrophy (FSHD): immunocytochemical and genetic analyses. *Muscle Nerve* 1995;**2**:S56–S66.
30. Dmitriev P, Kiseleva E, Kharchenko O, Ivashkin E, Pichugin A, Dessen P, et al. Dux4 controls migration of mesenchymal stem cells through the Cxcr4-Sdf1 axis. *Oncotarget* 2016;**7**:65090–65108.
31. Wallach D, Kang TB, Kovalenko A. Concepts of tissue injury and cell death in inflammation: a historical perspective. *Nat Rev Immunol* 2014;**14**:51–59.
32. Kowaljow V, Marcowycz A, Ansseau EN, Conde CB, Sauvage SB, Mattéotti C, et al. The DUX4 gene at the FSHD1A locus encodes a pro-apoptotic protein. *Neuromuscular disorders: NMD* 2007;**17**:611–623.
33. Wuebbles RD, Long SW, Hanel ML, Jones PL. Testing the effects of FSHD candidate gene expression in vertebrate muscle development. *Int J Clin Exp Pathol* 2010;**3**:386–400.
34. Shadle SC, Zhong JW, Campbell AE, Conerly ML, Jagannathan S, Wong CJ, et al. DUX4-induced dsRNA and MYC mRNA stabilization activate apoptotic pathways in human cell models of facioscapulohumeral dystrophy. *PLoS Genet* 2017;**13**:e1006658.
35. Winokur ST, Barrett K, Martin JH, Forrester JR, Simon M, Tawil R, et al. Facioscapulohumeral muscular dystrophy (FSHD) myoblasts demonstrate increased susceptibility to oxidative stress. *Neuromuscular disorders: NMD* 2003;**13**:322–333.
36. Bou Saada Y, Dib C, Dmitriev P, Hamade A, Carnac G, Laoudj-Chenivesse D, et al. Facioscapulohumeral dystrophy myoblasts efficiently repair moderate levels of oxidative DNA damage. *Histochem Cell Biol* 2016;**145**:475–483.
37. Dmitriev P, Bou Saada Y, Dib C, Ansseau E, Barat A, Hamade A, et al. DUX4-induced constitutive DNA damage and oxidative stress contribute to aberrant differentiation of myoblasts from FSHD patients. *Free Radic Biol Med* 2016;**99**:244–258.
38. Passerieux E, Hayot M, Jaussent A, Carnac G, Gouzi F, Pillard F, et al. Effects of vitamin C, vitamin E, zinc gluconate, and selenomethionine supplementation on

muscle function and oxidative stress biomarkers in patients with facioscapulohumeral dystrophy: a double-blind randomized controlled clinical trial. *Free Radic Biol Med* 2015;**81**:158–169.
39. Kelliher MA, Grimm S, Ishida Y, Kuo F, Stanger BZ, Leder P. The death domain kinase RIP mediates the TNF-induced NF-κB signal. *Immunity* 1998;**8**:297–303.
40. Choi ME, Price DR, Ryter SW, Choi AMK. Necroptosis: a crucial pathogenic mediator of human disease. *JCI Insight* 2019;**4**(15). https://doi.org/10.1172/jci.insight.128834
41. Von Haehling S, Morley JE, Coats AJS, Anker SD. Ethical guidelines for publishing in the Journal of Cachexia, Sarcopenia and Muscle: update 2019. *J Cachexia Sarcopenia Muscle* 2019;**10**:1143–1145.